
AutoV: Learning to Retrieve Visual Prompt for Large Vision-Language Models

Yuan Zhang^{1,2,*}, Chun-Kai Fan¹, Tao Huang³, Ming Lu^{1,*}, Sicheng Yu²,
Junwen Pan², Kuan Cheng¹, Qi She^{2,*}, Shanghang Zhang^{1,†}

¹School of Computer Science, Peking University, ²ByteDance, ³Shanghai Jiao Tong University

*Work done during ByteDance Internship, supervised by Qi She, *Project leaders, †Corresponding author

Abstract

Inspired by text prompts in large language models (LLMs), visual prompts have been explored to enhance the reasoning capabilities of large vision-language models (LVLMs). Current methods design heuristic visual prompts, such as overlaying a text-query-guided attention heatmap on the original input image. However, designing effective prompts manually is challenging and time-consuming, and it often fails to explore the benefits of different visual prompts, leading to sub-optimal performance. To this end, we propose **AutoV** that learns to automatically select the optimal visual prompt from various candidates based on given textual queries and the input image. To train AutoV, we developed an automatic data collection and labeling pipeline that evaluates various visual prompts with a pre-trained LVLm. We input a set of visual prompts into the LVLm and rank them according to the prediction losses generated by the model. Using the ranking as a supervision signal, we train AutoV to automatically choose the optimal visual prompt from various visual prompts for LVLms. Experimental results indicate that AutoV enhances the performance of various LVLms across multiple popular image understanding tasks. For instance, LLaVA-OV with AutoV achieves **1.7%** accuracy gain on LLaVA^{Wild}, and AutoV boosts Qwen2.5-VL by **1.9%** on MMMU, highlighting its potential as an optimal visual prompting method for LVLms.

Date: June 23, 2025

Correspondence: Shanghang Zhang at shanghang@pku.edu.cn

1 Introduction

Recent advancements in large language models (LLMs) [1, 8, 10, 37, 39, 47] have spurred significant progress in large vision-language models (LVLms), which connect visual encoders with language model decoders to effectively adapt textual reasoning capabilities to visual understanding tasks [4, 5, 13, 24–26, 31, 32]. Therefore, visual input plays a crucial role in LVLms, enabling precise perception and fine-grained grounding across various multimodal scenarios.

To further improve the perception and reasoning of LVLms, visual prompting [30, 43, 53, 55] has emerged as an important technique analogous to textual prompting in LLMs [22, 49, 65]. Visual prompts enhance model performance by adding visual annotations such as masks, colorful circles, or heatmaps, thus guiding the attention of LVLms toward crucial image regions of interest. However, existing visual prompting methods predominantly rely on heuristically designed prompts, limiting their ability to fully exploit the inherent diversity of visual prompts. As illustrated in Figure 1, we list the benchmark-level performance of existing heuristic

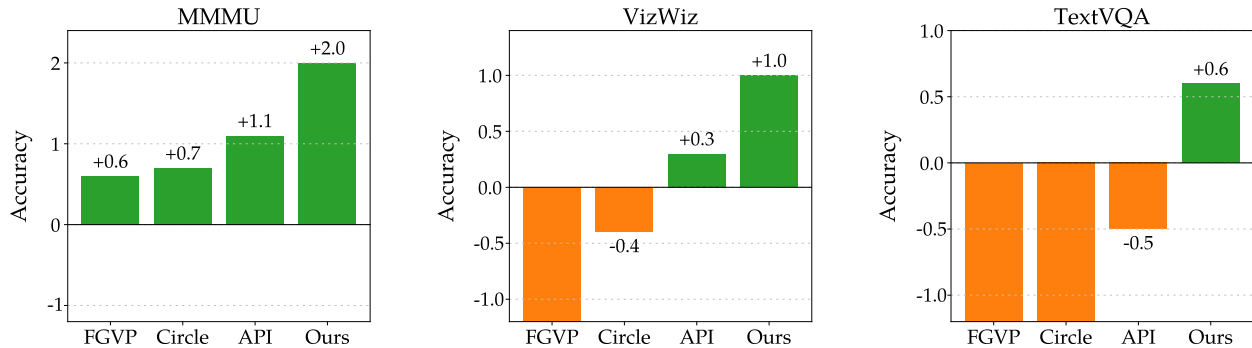


Figure 1 Benchmark-level evaluation within FGVP, Circle, API, and our AutoV. The above methods employ heuristic visual prompts: (1) FGVP applies blur effects, (2) Circle highlights foreground objects in red, and (3) API utilizes attention maps as masks. In contrast to existing methods, AutoV learns to retrieve the optimal visual prompt using a lightweight ranking network.

prompt methods (e.g., FGVP [53], Red Circle [43], and API [55]). While all three methods demonstrate effectiveness on logic-intensive MMMU tasks, both blur-based FGVP and bounding prompts adversely affect vision-centric benchmarks (e.g., VizWiz [9]) and OCR-dependent tasks (e.g., TextVQA [44]). This is because heuristic prompt methods fail to automatically tune hyperparameters for each benchmark or even each instance.

Hence, to develop a more effective visual prompt strategy suitable for diverse vision-language tasks, it is vital to adaptively retrieve the optimal visual prompt that most significantly improves the perception and reasoning of LVLMs in response to specific queries. Motivated by this, we introduce **AutoV**, an innovative visual prompting retrieval framework designed to dynamically select the optimal visual prompt from a diverse set of candidates, explicitly tailored to the textual query and input image. Specifically, we first generate a diverse set of visual prompt candidates¹ and encode their representation. This diversity enables the framework to capture distinct visual representations that may be optimal for various query-image pairs. Next, we design a lightweight ranking network that efficiently integrates visual and textual information to predict the rankings preferences over prompt candidates. Finally, the highest-ranking candidate is chosen as the input for LVLMs during inference.

To train the ranking network, we establish an automated pipeline for collecting and labeling training data, evaluating the rank of each visual prompt candidate based on the prediction losses of a pre-trained LVLm. Subsequently, the ranking network is supervised using a reward loss that differentiates between selected and rejected candidates. This strategy offers reliable supervision, allowing AutoV to attain adaptive, query-specific prompt retrieval without the need for extensive manual annotation.

AutoV achieves significant performance improvements across various prominent LVLm architectures and diverse image understanding benchmarks, including fine-grained comprehension, real-world visual assistance, and complex open-ended reasoning tasks. For instance, integrating AutoV with LLaVA-OneVision and InternVL2 leads to improvements of **1.7%** and **2.2%** on LLaVA^{Wild}, respectively. Additionally, AutoV enhances Qwen2.5-VL on MMMU by **1.9%**, highlighting its significant advantage in adaptive visual prompting retrieval. In summary, our contributions are as follows:

- We present AutoV, a novel automatic visual prompting framework for large vision-language models that adaptively retrieves the optimal visual prompt from a diverse candidate set, explicitly tailored to textual query and visual context pairs.
- We create a scalable and automated data collection pipeline equipped with a reward-based loss to effectively train a lightweight ranking network, facilitating accurate and adaptive visual prompt selection without the need for extensive manual annotations.
- We perform comprehensive experiments to validate the efficacy and generalizability of AutoV across

¹In this work, we use attention-based visual prompts from various transformer layers of CLIP in API [55].

various multimodal models and benchmarks, showcasing consistent and significant performance improvements over existing visual prompting methods. Once trained, AutoV integrates seamlessly into various LVLMs without additional fine-tuning.

2 Related Work

Large Vision-Language Models. Recent advances in large language models [1, 8, 10, 37, 39, 47] have catalyzed a new wave of large vision-language models [2, 4, 13, 25, 26, 31]. By coupling a high-capacity visual encoder with an LLM decoder, LVLMs transfer textual reasoning to visual understanding, and the quality of input images determines the lower bound of multimodal abilities. For instance, the popular LLaVA-OneVision [24] and Qwen2.5-VL [5] adopt a higher and dynamic resolution recipe for training to enhance their fine-grained reasoning, while vision-centric scaling in InternVL2 [11] enlarges the ViT [15] backbone to boost grounding capability. However, the above methods require training times of several hundred GPU days. Here, *can we further boost the existing LVLMs by optimizing the visual input itself during the inference stage?* The answer is *Yes*. Visual prompting [29, 45] is an emerging and effective technique in this direction.

Visual Prompting for LVLMs. LVLMs relying solely on textual inputs exhibited two key limitations: visual hallucinations [6, 18] and language-driven biases [38, 50]. To better mitigate these challenges, visual prompting [29, 45, 51, 60] has emerged as an alternative way of supplying cues in the visual modality. Compared with textual prompts, it is more concise and explicit, while allowing guidance that reaches fine-grained, pixel-level details. Early work [43] shows that simply drawing a red circle around a target object steers CLIP [40] attention, yielding great performance on referring-expression and keypoint-localization benchmarks. FGVP [53] extends this idea with fine-grained prompting, replacing coarse shapes with blur-reversal prompts based on segmentation masks, further improving accuracy on RefCOCO [61]. AlphaCLIP [45] trains an augmented version of CLIP with an auxiliary alpha channel for indicating regions at the expense of increased training overhead. API [55] proposes attention prompting on images, overlaying text-guided attention heatmaps, boosting LVLMs on VQA, and open-ended reasoning tasks. *Although previous studies have explored various visual prompts, it remains unclear which prompt is optimal for a specific image-question pair, leading to a decrease in the practicability of visual prompts.* To address this limitation, we introduce our visual prompting method that learns to retrieve the optimal visual prompt for a specific image-question pair.

Visual Retrieval for LVLMs. A variety of strategies have been proposed for visual retrievals, such as visual token selection [12, 54, 63] for LVLMs. Existing visual prompt selection pipelines generally adhere to three main paradigms. (1) The heuristic paradigm identifies benchmark-level optimal parameters through extensive evaluation but lacks instance-specific adaptation. (2) The random paradigm offers a stochastic baseline characterized by instance-level variation, but it lacks performance guarantees. This establishes it as the lower bound for adaptive approaches. (3) The Mixture-of-Experts (MoE) paradigm [7, 16, 66] provides the most direct form of adaptation by utilizing the GateNet specifically for visual retrieval. However, MoE gates are susceptible to overfitting during training, which can result in poor generalization. To mitigate these limitations, we propose an efficient ranking network specifically designed for visual retrieval, which models the pairwise preference ordering.

3 Proposed Approach: AutoV

In this section, we present AutoV for optimal visual prompt retrieval. Our framework includes four critical components: (1) feature extraction of prompt candidates, (2) candidate ranking consisting of modality interaction and single-modality mapping modules, (3) reward loss supervision along with automated data generation, and (4) an efficient inference pipeline. The overall architecture is illustrated in Figure 2, where the four modules are color-coded for clarity. Best viewed in color.

3.1 Feature Extraction of Prompt Candidates

The primary goal is to effectively choose the most appropriate visual prompt in response to various text queries and input images. For a group of n input visual prompts $\{x_1, x_2, \dots, x_n\}$, we employ a visual encoder

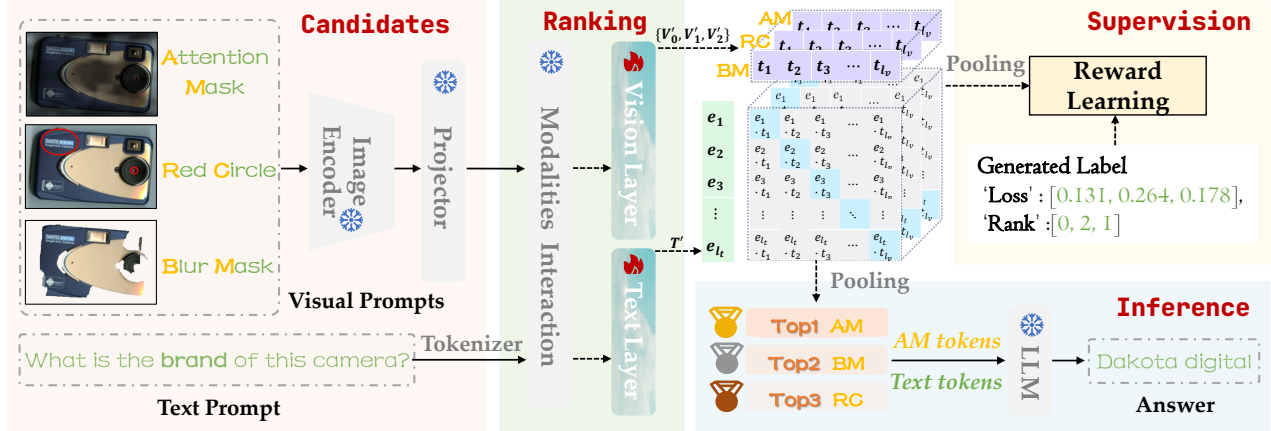


Figure 2 The illustration of AutoV. It comprises four key components: representation extraction from candidates, ranking network for reward score, reward-supervised training, and inference. The framework aims to retrieve the most suitable visual prompt tailored to each query-image pair.

$g(\cdot)$ (e.g., like CLIP [40]) to generate the visual feature:

$$\mathbf{Z}_i = g(x_i) \text{ with } i \in \{1, \dots, n\}. \quad (1)$$

Next, we apply a projection matrix \mathbf{W} to transform each visual feature \mathbf{Z}_i into language embedding tokens $\mathbf{V}_i = \mathbf{W} \times \mathbf{Z}_i$, aligning the same dimensionality as the word embedding space in the language model. As a result, we obtain a set of visual candidates represented in the form of visual tokens $\mathbf{V}_i \in \mathbb{R}^{L \times D}$ to rank, where L denotes the length of vision tokens and D is the language embedding dimension. Notably, both the visual encoder and the alignment projector are directly inherited from a fully trained LVLM, and we adopt them without any additional fine-tuning.

3.2 Candidate Ranking Network

The goal of the ranking network is to effectively rank the visual prompt candidates based on their relevance to the textual query, by modeling the relationship between the visual tokens and the input text. Therefore, we first propose the modality interaction module to enable visual tokens to fuse the context information of text tokens. Inspired by observations in [62] that modality-fusion occurs in the early layers of the LLM, we use the first layer of the LLM decoder $f(\cdot)$ for modality interaction. Thus visual candidate tokens \mathbf{V}_i and text tokens \mathbf{T} are concatenated and fed into the interaction module:

$$\mathbf{H}_i = f(\text{concat}(\mathbf{V}_i, \mathbf{T})), \quad (2)$$

with the outputs are $\tilde{\mathbf{V}}_i = \mathbf{H}_i[:l_v]$ and $\tilde{\mathbf{T}} = \prod_i \mathbf{H}_i[-l_t:]$. Next, we input visual candidate tokens $\tilde{\mathbf{V}}_i$ into a vision mapping module, which is implemented using a feed-forward network (FFN). The generated final candidate features are $\mathbf{V}'_i \in \mathbb{R}^{l_v \times h}$, where $h \ll D$ is the output dimension of the vision mapping module to save computational cost. Besides, the query tokens $\tilde{\mathbf{T}}$ are also converted by a text mapping module to get the query embeddings $\mathbf{T}' \in \mathbb{R}^{l_t \times h}$. In AutoV, we define visual retrieval as a customized ranking task rather than a classification or regression problem, and the reason is discussed in Section 3.3. Therefore, we calculate the reward scalar for given visual candidate tokens \mathbf{V}'_i , where the context similarity with the query serves as the quantitative target. We utilize a cross-attention operation to achieve:

$$s(\text{VP}_i) = \text{mean}(\text{cross-attn}(\mathbf{V}'_i, \mathbf{T}')). \quad (3)$$

Here, only the vision and text mapping modules need additional training, each consisting of a single FFN with two linear layers. The total parameters are $2h(D + h + 2)$, resulting in lower training costs.

3.3 Reward Loss Supervision

Automated Data Generation. We create customized data to train the ranking network to select the optimal visual prompt for a given LVLM. Our approach is grounded in a simple intuition: *a superior visual prompt should yield lower language modeling loss when input into any trained LVLM*. We optimize the ranking network using relative loss instead of a one-hot selection vector, as correctness can stem from the LVLM’s language priors without relying on any input content [52, 56]. In contrast, the inference loss indicates the confidence of models in generating answers based on the input visual-question pair: *a lower loss indicates higher confidence* [17, 64].

For each group of n visual candidates, we generate n (VP, query) pairs and comprehensively evaluate them. Each pair is processed by a fully trained vision-language model to compute its combination loss, defined as the modeling loss relative to the ground truth, and sorted to get a rank. To ensure high-quality ranking data, we implement two filtering criteria for (VP, query) pairs: (1) we remove pairs exhibiting low loss variance, as their insensitivity to visual prompts suggests answers are generated from the language priors rather than actual input content; (2) we exclude pairs with excessively high average loss, which indicates outlier case or weak visual prompt-query correlation.

For each raw (image, query) pair, we generate a training sample structured as a **quadruple**:

$$\langle \text{query}, \{vp_0, vp_1, \dots, vp_{n-1}\}, \text{rank}, \text{reward loss} \rangle,$$

with an illustrative example provided in Figure 2, and the dataset we adopt is detailed in Appendix B.

Reward Loss Supervision. Inspired by the reward modeling from human feedback in OpenAI [36], we train our ranking network using reward modeling to align its partial order with the optimal visual prompt. Here, we model visual retrieval as a customized ranking task rather than a classification or regression problem. This is because the objective is not to assign absolute labels or scores, but to identify the most appropriate prompt from a set of candidates by comparing their relative effectiveness in enhancing multimodal understanding. Ranking allows the model to learn fine-grained preferences across diverse query-image combinations and better align with the real-world setting.

In Figure 3, we pair all n visual prompt candidates exhaustively, ensuring each prompt is combined with every other prompt exactly once. This results in generating $\mathcal{C}(n, 2)$ training pairs for each instance. The reason is that, unlike pointwise scoring, which assigns low scores to all responses for inherently challenging tasks, pairwise comparison allows for finer discrimination between responses. Based on the rank and loss from the quadruples, we reinforce the visual prompt with lower loss (chosen sample) for each pair, while penalizing the higher-loss visual prompt (rejected sample).

Specifically, the reward loss \mathcal{L}_r is designed as:

$$\mathcal{L}_r = -\frac{1}{\mathcal{C}(n, 2)} \mathbb{E} \left[\log \left(\sigma \left(s(\text{VP}_c) - s(\text{VP}_r) \right) \right) \right], \quad (4)$$

where $s(\text{VP}_c)$ is the scalar output of the ranking network for the chosen visual prompt out of the pair, $s(\text{VP}_r)$ represents the rejected one, and σ denotes the Sigmoid function.

3.4 Efficient Inference Pipeline

During the inference stage, we input several suitable visual prompt candidates along with the query into the large vision-language model and then pass them through our ranking network, as illustrated in Figure 2. Next, the ranking network outputs the corresponding reward scalar of each visual prompt. We then select the highest-scoring visual prompt, concatenate its visual tokens with text embeddings, and decode their representation through the LLM to produce the final answer.

4 Experiments

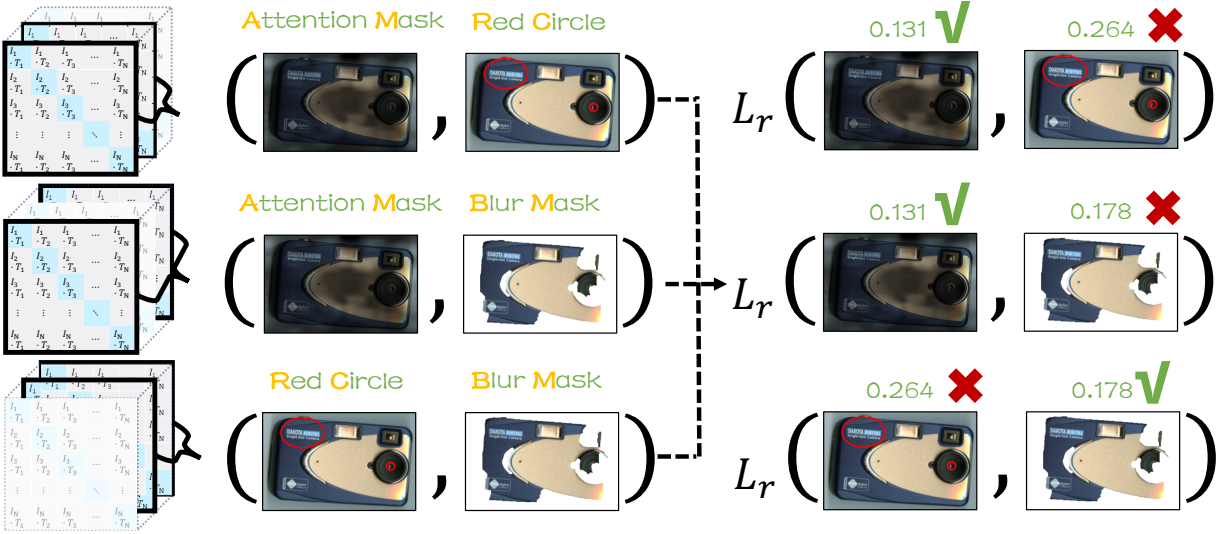


Figure 3 The reward loss of AutoV. As a concrete example, we illustrate the pairwise combination process using the visual prompts from Figure 2, demonstrating how our supervision is applied.

4.1 Experiment Settings

Models. We apply our AutoV to four mainstream open-source large vision-language models, i.e., LLaVA-v1.5 [33], LLaVA-OneVision [24], Qwen2.5-VL [5], and InternVL2 [14]. In particular, LLaVA-v1.5 employs CLIP-pretrained ViT [40] as the visual tower and Llama2 [48] as the LLM backbone. LLaVA-OneVision enhances this design with SigLIP [59] for high-resolution refinement and replaces the LLM with Qwen2 [3]. Qwen2.5-VL features a dynamic resolution encoder, while InternVL2 adopts InternViT [13] for visual encoding and InternLM2 [11] as its LLM decoder.

Benchmarks. We evaluate AutoV on six widely-adopted image understanding benchmarks, including MMMU [58], POPE [27], VizWiz [9], MMVet [57], VQA^{Text} (TextVQA) [44], and LLaVA^{Wild} (LLaVA-Bench in-the-wild) [31]. The evaluation benchmarks contain various aspects: hallucination suppression (POPE), STEM reasoning (MMMU), real-world visual assistance (VizWiz), fine-grained comprehension (MMVet), text-rich understanding (VQA^{Text}), and open-world reasoning (LLaVA^{Wild}).

4.2 Main Results

Our results are listed in Table 1, and we compare AutoV with three previous visual prompting methods designed for LVLMs, including FGVP [53], RedCircle [43], and API [55]. Performance improvements and decrements listed in the table are calculated relative to the base model. The training data and implementation details can be found in Appendix B and D.

The main observations from the experimental results are as follows: (1) AutoV significantly outperforms existing methods, demonstrating consistent advantages across all models and benchmarks. Specifically, for LLaVA-7B, LLaVA-13B, LLaVA-OneVision, InternVL2, and Qwen2.5-VL, the average improvements relative to the base model are 1.3%, 1.4%, 1.1%, 0.9% and 0.9%, respectively. Our method performs particularly well for LLaVA-7B on MMVet, with an improvement of 2.2%. Excluding it, our method appears more effective and robust on the VQA^{Text} task, where other methods all fail to achieve positive gain. (2) Our approach shows the most significant performance advantage on MMVet compared to the API. With an average score of 1.4% for our method versus 0.1% for theirs, the relative difference of 1.3% underscores the importance of accurate case-level visual cues retrieval instead of benchmark-level visual prompts selection. The other two visual prompting methods, lacking the ability to adapt to different queries, do not perform well on VQA tasks. (3) Our method further supplements inherently less accurate models. For instance, LLaVA-7B equipped with our approach, achieves higher accuracy on the MMMU and POPE tasks than the 13B-scale model. This means that our method can be utilized for model efficiency on certain specific tasks: a few additional MLP

Table 1 Comparison of AutoV with other visual prompts methods for various LVLMs. The numbers in parentheses denote the performance difference relative to the **Base Model** accuracy: **red** indicates a decrease, while **green** indicates an improvement. The final column reports the average performance gain of methods across LVLMs. The percentage symbol (%) is omitted for brevity.

Method	MMMU	POPE	VizWiz	MMVet	VQA ^{Text}	LLaVA ^{Wild}	Avg.
LLaVA-v1.5 (7B)							
Base Model	36.3	85.9	50.0	30.6	58.2	65.4	(−0.0)
FGVP (NIPS23)	36.9 (↑ 0.6)	72.6 (↓ 13.3)	47.5 (↓ 2.5)	29.0 (↓ 1.6)	46.3 (↓ 11.9)	55.6 (↓ 9.8)	(↓ 6.4)
Circle (ICCV23)	37.0 (↑ 0.7)	84.5 (↓ 1.4)	49.6 (↓ 0.4)	31.3 (↑ 0.7)	55.5 (↓ 2.7)	62.2 (↓ 3.2)	(↓ 1.1)
API (ECCV24)	37.4 (↑ 1.1)	86.0 (↑ 0.1)	50.3 (↑ 0.3)	31.8 (↑ 1.2)	57.7 (↓ 0.5)	65.8 (↑ 0.4)	(↑ 0.4)
AutoV	38.3 (↑ 2.0)	86.8 (↑ 0.9)	51.0 (↑ 1.0)	32.8 (↑ 2.2)	58.8 (↑ 0.6)	66.6 (↑ 1.2)	(↑ 1.3)
LLaVA-v1.5 (13B)							
Base Model	36.7	85.9	53.6	36.1	61.2	66.6	(−0.0)
FGVP (NIPS23)	36.9 (↑ 0.2)	66.8 (↓ 19.1)	46.8 (↓ 6.8)	29.7 (↓ 6.4)	49.2 (↓ 12.0)	63.7 (↓ 2.9)	(↓ 7.8)
Circle (ICCV23)	36.9 (↑ 0.2)	84.6 (↓ 1.3)	53.8 (↑ 0.2)	31.2 (↓ 4.9)	58.1 (↓ 3.1)	66.9 (↑ 0.3)	(↓ 1.4)
API (ECCV24)	37.3 (↑ 0.6)	85.6 (↓ 0.3)	54.6 (↑ 1.0)	35.6 (↓ 0.5)	60.6 (↓ 0.6)	67.6 (↑ 1.0)	(↑ 0.2)
AutoV	38.5 (↑ 1.8)	86.9 (↑ 1.0)	55.4 (↑ 1.8)	37.0 (↑ 0.9)	61.9 (↑ 0.7)	68.5 (↑ 1.9)	(↑ 1.4)
LLaVA-OneVision (7B)							
Base Model	49.4	89.1	58.2	48.8	76.1	80.6	(−0.0)
FGVP (NIPS23)	48.6 (↓ 0.8)	82.9 (↓ 6.2)	52.0 (↓ 6.2)	45.5 (↓ 3.3)	65.4 (↓ 10.7)	70.8 (↓ 9.8)	(↓ 5.9)
Circle (ICCV23)	48.4 (↓ 1.0)	88.2 (↓ 0.9)	59.6 (↑ 1.4)	47.2 (↓ 1.6)	73.0 (↓ 3.1)	76.9 (↓ 3.7)	(↓ 1.5)
API (ECCV24)	49.0 (↓ 0.4)	88.9 (↓ 0.2)	58.7 (↑ 0.5)	48.1 (↓ 0.7)	75.9 (↓ 0.2)	80.9 (↑ 0.3)	(↓ 0.1)
AutoV	50.0 (↑ 0.6)	90.0 (↑ 0.9)	59.4 (↑ 1.2)	49.9 (↑ 1.1)	77.3 (↑ 1.2)	82.3 (↑ 1.7)	(↑ 1.1)
InternVL2 (8B)							
Base Model	48.6	87.8	58.6	46.5	77.0	74.6	(−0.0)
FGVP (NIPS23)	47.2 (↓ 1.4)	84.2 (↓ 3.6)	52.3 (↓ 6.3)	36.8 (↓ 9.7)	70.7 (↓ 6.3)	70.2 (↓ 4.4)	(↓ 5.3)
Circle (ICCV23)	48.3 (↓ 0.3)	86.0 (↓ 1.8)	57.5 (↓ 1.1)	40.3 (↓ 6.2)	74.9 (↓ 2.1)	74.0 (↓ 0.6)	(↓ 2.0)
API (ECCV24)	48.3 (↓ 0.3)	87.9 (↑ 0.1)	58.0 (↓ 0.6)	46.3 (↓ 0.2)	77.0 (−0.0)	75.6 (↑ 1.0)	(−0.0)
AutoV	49.2 (↑ 0.6)	88.5 (↑ 0.7)	59.1 (↑ 0.5)	47.2 (↑ 0.7)	77.9 (↑ 0.9)	76.8 (↑ 2.2)	(↑ 0.9)
Qwen2.5-VL (7B)							
Base Model	50.1	87.5	69.5	56.6	83.0	98.0	(−0.0)
FGVP (NIPS23)	49.6 (↓ 0.5)	81.6 (↓ 5.9)	65.8 (↓ 3.7)	43.1 (↓ 13.5)	78.0 (↓ 5.0)	90.4 (↓ 7.6)	(↓ 6.0)
Circle (ICCV23)	48.2 (↓ 1.9)	84.2 (↓ 3.3)	66.7 (↓ 2.8)	44.5 (↓ 12.1)	80.5 (↓ 2.5)	89.5 (↓ 8.5)	(↓ 5.2)
API (ECCV24)	51.0 (↑ 0.9)	87.6 (↑ 0.1)	69.3 (↓ 0.2)	56.8 (↑ 0.2)	82.3 (↓ 0.7)	98.1 (↑ 0.1)	(↑ 0.1)
AutoV	52.0 (↑ 1.9)	88.1 (↑ 0.6)	70.0 (↑ 0.5)	57.6 (↑ 1.0)	83.4 (↑ 0.4)	98.8 (↑ 0.8)	(↑ 0.9)

layers are a better choice compared with hundreds of times larger in parameter size. (4) Both Qwen2.5-VL and InternVL2 integrate the retrieval-augmented prompting strategy from AutoV, which is pre-trained on LLaVA-OneVision. This integration results in an average accuracy gain of 0.9%. Notably, the improvements are consistent and observed in all individual tasks, including complex reasoning (e.g., MMVet) and real-world scenarios (e.g., VizWiz). This demonstrates that the effectiveness of the retrieval-enhanced prompting strategy is model-agnostic and generalizes well across heterogeneous LVLm architectures, regardless of pretraining scales or backbone variations.

4.3 Ablation Study

4.3.1 How does ranking compare to other retrieval methods?

To better analyze why ranking is more suitable for retrieving visual prompts, we list three other retrieval methods and provide experimental evidence for comparison, including heuristic retrieval, random retrieval, and mixture-of-experts retrieval. All experiments are conducted on LLaVA-v1.5.

Heuristic Fixed Retrieval. Heuristic retrieval only involves a single fixed type of visual prompts, e.g., red circle [43], or attention image [55], based on its predefined rules or heuristics. Furthermore, to identify the best rules, they need to conduct benchmark-level multiple rounds of trials, consuming a significant amount of reasoning resources. As shown in rows 3 to 6 of Table 2, we find that each visual prompt could potentially be the optimal solution for different benchmarks. For instance, VP_3 achieves the best results on MMMU, while VP_1 is optimal on MMVet, and there is a significant variation in the performance of different types of visual prompts across various benchmarks. *In summary, heuristic retrieval offers simplicity in retrieval processes*

Table 2 The analysis between our method and other retrieval methods.

Method	MMMU	VizWiz	MMVet	Avg.
Baseline	36.3	50.0	30.6	39.0 (−0.0)
VP ₁ only	36.5 (+0.2)	50.0 (−0.0)	31.8 (+1.2)	39.4 (+0.4)
VP ₂ only	36.9 (+0.6)	50.3 (+0.3)	31.2 (+0.6)	39.5 (+0.5)
VP ₃ only	37.4 (+1.1)	49.9 (−0.1)	31.7 (+1.1)	39.7 (+0.7)
VP ₄ only	37.1 (+0.8)	50.3 (+0.3)	30.8 (+0.2)	39.7 (+0.7)
Random	37.2 (+0.9)	50.4 (+0.4)	31.6 (+1.0)	39.7 (+0.7)
Mixture-of-Experts	37.6 (+1.3)	50.4 (+0.4)	31.7 (+1.1)	39.9 (+0.9)
AutoV	38.3 (+2.0)	51.0 (+1.0)	32.8 (+2.2)	40.7 (+1.7)

with the need for conducting benchmark-level multiple rounds of trials.

Random Retrieval. Random retrieval picks up one visual prompt from the candidate pool without any specific criteria or order. The 7th row of Table 2 lists its results, comparing with the individual visual prompt, we observe that the random retrieval’s performance is on par with or slightly superior across the three benchmarks. For instance, the random algorithm outperforms VP₁ in MMMU by 0.7%, VP₂ in MMVet by 0.5%, and even surpasses the best results of the VP candidates in VizWiz. *The above experiment demonstrates that by flexibly selecting from multiple visual prompt candidates, even random retrieval has the potential to outperform individual visual prompts, and the conclusion provides valuable insights for our approach.*

MoE (or GateNet) Retrieval. Mixture-of-experts (MoE) retrieval is a prevalent technique used to identify the most relevant expert for a model decision-making process, where the Gumbel Softmax function is employed to assign weights to the GateNet in a differentiable manner during training [16]. In our scenario, the features of multiple visual prompts are input to GateNet to determine which one should be retained and fed into the LLM. We insert GateNet into the output of the projection layer and train it with the same amount of data and training time as AutoV. The results can be seen in the 8th row of Table 2. We observe a 0.9% improvement with MoE compared to the baseline. However, the improvement compared to the random algorithm was only 0.2%, lagging significantly behind AutoV by 0.8%. We suspect that the Mixture-of-Experts architecture encounters a lack of generalization ability during the fine-tuning stage, which can easily lead to overfitting. Additionally, this architecture does not incorporate textual modality for guidance. *Therefore, MoE retrieval may not be the optimal approach for visual prompt retrieval in LVLMS. It is important to adopt a more robust framework that integrates textual guidance to enhance overall performance effectively.*

Retrieval Visualization. We visualize the prompt distribution of retrieval strategies in practical tasks. Taking the MMVet task as an example, Figure 4 presents a bar graph comparing the retrieval decisions of GateNet and our AutoV. The bar heights indicate the frequency of visual prompt retrieval, while the overlaid line plots depict the independent accuracy for each prompt. Our analysis reveals a notable discrepancy between the GateNet retrieval strategy and the actual inference accuracy of visual prompts. For instance, GateNet retrieves VP₃, the second-most useful prompt, only 38 times (28/218, 12.8% of cases), despite its high accuracy. In contrast, AutoV exhibits stronger alignment with the standalone accuracy of visual prompts, and prefers to select VP₁ and VP₃, the two prompts that own superior accuracy.

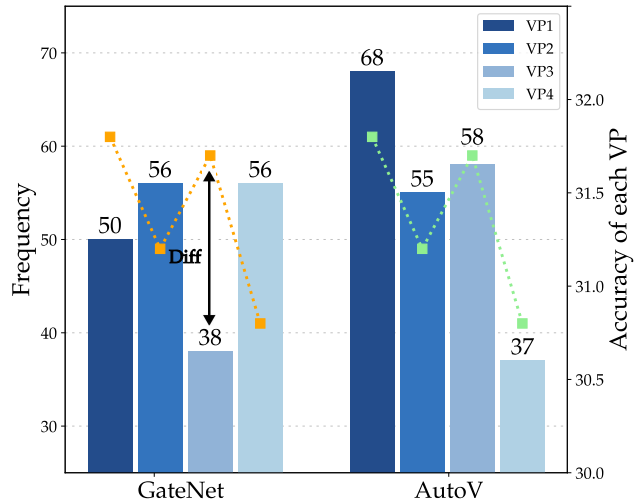


Figure 4 Retrieval distribution on MMVet. The plots are independent accuracy for each prompt.

Table 3 The performance comparison of different numbers of visual prompts in AutoV. 0 visual prompts represent the original image input, while 2-6 visual prompts are from attention prompting images [55] from different layers. On the other hand, 7 and 8 visual prompts are generated based on the former by incorporating prompts generated using the Redcircle [43] and FGVP [53], respectively.

Number	Source	MMMU	VizWiz	MMVet	Avg.
0	Vanilla image	36.3	50.0	30.6	39.0 (−0.0)
2	+ {L22, L23}	37.3 (+1.0)	50.3 (+0.3)	32.0 (+1.4)	39.9 (+0.9)
3	+ {L20}	37.8 (+1.5)	50.8 (+0.8)	32.3 (+1.7)	40.3 (+1.3)
4	+ {L15}	38.3 (+2.0)	51.0 (+1.0)	32.8 (+2.2)	40.7 (+1.7)
5	+ {L19}	38.2 (+1.9)	50.8 (+0.8)	32.8 (+2.2)	40.6 (+1.6)
6	+ {L21}	38.5 (+2.2)	50.7 (+0.7)	32.6 (+2.0)	40.6 (+1.6)
7	+ {RedCircle}	38.7 (+2.4)	50.7 (+0.7)	32.9 (+2.3)	40.8 (+1.8)
8	+ {FGVP}	38.7 (+2.4)	50.4 (+0.4)	32.4 (+1.8)	40.5 (+1.5)

4.3.2 More candidates perform better?

In AutoV, having more visual prompt candidates can offer a more diverse selection, enhancing the flexibility and adaptability of LVLMs. *However, is it always better to have more visual prompts?* In the main experiment, we used the attention prompting images [55] from layers 15, 20, 22, and 23 in the CLIP [40] model as inputs, with a total of 4 visual prompts. Here, we consider extra scenarios ranging from 2 ~ 8 prompts and conduct experiments on the MMMU, VizWiz, and MMVet benchmarks. The results are listed in Table 3. First, we observe that when the visual prompts themselves can lead to performance improvement, the accuracy increases as their quantity grows, but the rate of accuracy improvement slows down as the number continues to rise. Taking the experiments on MMMU as an example, as the number of prompts increases, the performance gain remains at 0.5% when increasing from 2 to 4 prompts. However, when further increasing 7 to 8 prompts, the improvement drops to 0, even though FGVP alone can contribute a 0.6% gain. Then, even if a single visual prompt itself degrades accuracy, incorporating it into the candidate pool only marginally harms the overall performance, thanks to the inherent retrieval capability of AutoV. Taking the results on VizWiz as an example: although both RedCircle and FGVP individually show negative gains (−0.4% and −2.5% respectively), including them results in either no overall accuracy drop or just a minimal 0.3% decrease. In summary, both the quality and quantity of visual prompts impact overall performance. We recommend selecting known high-quality visual prompts as candidates, while limiting to fewer than 5 instances to strike the balance between accuracy and efficiency.

4.3.3 The transferability of AutoV

The retrieval strategy in our AutoV, trained on one LVLm, can be transferred to various other LVLms. First, our method demonstrates broad applicability across open-source models. In Table 1, both InternVL2 and Qwen2.5-VL achieve a 0.9% improvement by directly adopting the retrieval strategy from AutoV pre-trained on LLaVA-OneVision. More remarkably, Table 4 reveals that even closed-source models like Gemini-Pro [46] and GPT-4o [20] show substantial gains, averaging 6.4 and 6.0 points respectively. *Therefore, AutoV owns good transferability, as its retrieval strategy consistently boosts performance across both open- and closed-source LVLms without model-specific adaptation.*

Table 4 The performance of closed-source models with retrieval generated by AutoV.

Models	VizWiz	LLaVA
Gemini-1.5-Pro	45.9	77.9
+AutoV	55.5 (+9.6)	81.1 (+3.2)
GPT-4o	52.8	68.0
+AutoV	61.8 (+9.0)	70.9 (+2.9)
Qwen-VL-Max	64.6	85.8
+AutoV	71.9 (+7.3)	88.4 (+2.6)

4.3.4 The Efficiency of AutoV

While we enhance LVLm performance through AutoV, we uphold efficiency optimizations to ensure practicality. Initially, training a high-quality AutoV on the LLaVA-7B model within 40 epochs only requires 6 hours



Figure 5 Visualization of retrieved visual prompts on different queries. The VQA case is sampled in the LLaVA Bench. VP₁ and VP₃ come from API, VP₂ is from Circle, and VP₄ is from FGVP.

utilizing 8 NVIDIA A100-40GB GPUs. Furthermore, because of its transferability, training additional AutoV instances for each vision-language model is unnecessary, and we can generate the training samples via smaller models. Lastly, although AutoV introduces minimal additional FLOPs during inference (e.g., multiple image pre-processing and visual feature extraction), we can reduce latency by downsizing the final similarity matrix and single-prompt selection before LLM processing. As a result, the inference latency of the LLaVA-7B model increases by just 6.4 ms (from 254.8 ms to 261.2 ms), while yielding a 1.3% gain in average accuracy.

4.3.5 Qualitative Visualization

To further validate the effectiveness of our retrieval strategy, we visualize an example sourced from LLaVA-Bench. As shown in Figure 5, we list the output results of AutoV when we enter different queries. When faced with a question that focuses on the global context information, AutoV chooses VP₁ where the black mask removes the background. While referring to the "intended effect" in the image, AutoV selects VP₂, which directly uses red circles to highlight the weird spots. More visualization retrieval cases can be found in the Appendix G.2.

5 Conclusion

In this paper, we introduced AutoV, an adaptive visual prompting framework designed to effectively retrieve optimal visual prompts tailored to textual queries and image contexts for large vision-language models (LVLMs). By leveraging a lightweight ranking network trained via a reward-based supervision strategy, AutoV significantly surpasses existing heuristic prompting methods. Extensive experiments across multiple LVLM architectures and benchmarks demonstrate consistent improvements. Future research could explore integrating AutoV with more advanced prompt generation techniques or extending its framework to broader multimodal contexts beyond vision-language scenarios.

References

- [1] Josh Achiam, Steven Adler, Sandhini Agarwal, Lama Ahmad, Ilge Akkaya, Florencia Leoni Aleman, Diogo Almeida, Janko Altenschmidt, Sam Altman, Shyamal Anadkat, et al. Gpt-4 technical report. [arXiv:2303.08774](#), 2023.
- [2] Jean-Baptiste Alayrac, Jeff Donahue, Pauline Luc, Antoine Miech, Iain Barr, Yana Hasson, Karel Lenc, Arthur Mensch, Katherine Millican, Malcolm Reynolds, et al. Flamingo: a visual language model for few-shot learning. *Advances in neural information processing systems*, 35:23716–23736, 2022.
- [3] Jinze Bai, Shuai Bai, Yunfei Chu, Zeyu Cui, Kai Dang, Xiaodong Deng, Yang Fan, Wenbin Ge, Yu Han, Fei Huang, et al. Qwen technical report. [arXiv:2309.16609](#), 2023.
- [4] Jinze Bai, Shuai Bai, Shusheng Yang, Shijie Wang, Sinan Tan, Peng Wang, Junyang Lin, Chang Zhou, and Jingren Zhou. Qwen-VL: A frontier large vision-language model with versatile abilities. [arXiv:2308.12966](#), 2023.
- [5] Shuai Bai, Keqin Chen, Xuejing Liu, Jialin Wang, Wenbin Ge, Sibao Song, Kai Dang, Peng Wang, Shijie Wang, Jun Tang, et al. Qwen2. 5-vl technical report. [arXiv preprint arXiv:2502.13923](#), 2025.
- [6] Zechen Bai, Pichao Wang, Tianjun Xiao, Tong He, Zongbo Han, Zheng Zhang, and Mike Zheng Shou. Hallucination of multimodal large language models: A survey. [arXiv preprint arXiv:2404.18930](#), 2024.
- [7] Hangbo Bao, Wenhui Wang, Li Dong, Qiang Liu, Owais Khan Mohammed, Kriti Aggarwal, Subhojit Som, Songhao Piao, and Furu Wei. Vlmo: Unified vision-language pre-training with mixture-of-modality-experts. *Advances in Neural Information Processing Systems*, 35:32897–32912, 2022.
- [8] Xiao Bi, Deli Chen, Guanting Chen, Shanhuang Chen, Damai Dai, Chengqi Deng, Honghui Ding, Kai Dong, Qiu Shi Du, Zhe Fu, et al. Deepseek LLM: Scaling open-source language models with longtermism. [arXiv:2401.02954](#), 2024.
- [9] Jeffrey P Bigham, Chandrika Jayant, Hanjie Ji, Greg Little, Andrew Miller, Robert C Miller, Robin Miller, Aubrey Tatarowicz, Brandyn White, Samuel White, et al. Vizwiz: nearly real-time answers to visual questions. In *Proceedings of the 23rd annual ACM symposium on User interface software and technology*, pages 333–342, 2010.
- [10] Tom Brown, Benjamin Mann, Nick Ryder, Melanie Subbiah, Jared D Kaplan, Prafulla Dhariwal, Arvind Neelakantan, Pranav Shyam, Girish Sastry, Amanda Askell, et al. Language models are few-shot learners. *Advances in neural information processing systems*, 2020.
- [11] Zheng Cai, Maosong Cao, Haojiang Chen, Kai Chen, Keyu Chen, Xin Chen, Xun Chen, Zehui Chen, Zhi Chen, Pei Chu, et al. Internlm2 technical report. [arXiv preprint arXiv:2403.17297](#), 2024.
- [12] Liang Chen, Haozhe Zhao, Tianyu Liu, Shuai Bai, Junyang Lin, Chang Zhou, and Baobao Chang. An image is worth 1/2 tokens after layer 2: Plug-and-play inference acceleration for large vision-language models. In *European Conference on Computer Vision*, pages 19–35. Springer, 2024.
- [13] Zhe Chen, Jiannan Wu, Wenhui Wang, Weijie Su, Guo Chen, Sen Xing, Muyan Zhong, Qinglong Zhang, Xizhou Zhu, Lewei Lu, Bin Li, Ping Luo, Tong Lu, Yu Qiao, and Jifeng Dai. InternVL: Scaling up vision foundation models and aligning for generic visual-linguistic tasks. [arXiv:2312.14238](#), 2023.
- [14] Zhe Chen, Weiyun Wang, Yue Cao, Yangzhou Liu, Zhangwei Gao, Erfei Cui, Jinguo Zhu, Shenglong Ye, Hao Tian, Zhaoyang Liu, et al. Expanding performance boundaries of open-source multimodal models with model, data, and test-time scaling. [arXiv preprint arXiv:2412.05271](#), 2024.
- [15] Alexey Dosovitskiy, Lucas Beyer, Alexander Kolesnikov, Dirk Weissenborn, Xiaohua Zhai, Thomas Unterthiner, Mostafa Dehghani, Matthias Minderer, Georg Heigold, Sylvain Gelly, et al. An image is worth 16x16 words: Transformers for image recognition at scale. [arXiv preprint arXiv:2010.11929](#), 2020.
- [16] William Fedus, Barret Zoph, and Noam Shazeer. Switch transformers: Scaling to trillion parameter models with simple and efficient sparsity. *Journal of Machine Learning Research*, 23(120):1–39, 2022.
- [17] Chuan Guo, Geoff Pleiss, Yu Sun, and Kilian Q Weinberger. On calibration of modern neural networks. In *International conference on machine learning*, pages 1321–1330. PMLR, 2017.
- [18] Wen Huang, Hongbin Liu, Minxin Guo, and Neil Zhenqiang Gong. Visual hallucinations of multi-modal large language models. [arXiv preprint arXiv:2402.14683](#), 2024.

- [19] Drew A Hudson and Christopher D Manning. Gqa: A new dataset for real-world visual reasoning and compositional question answering. In Proceedings of the IEEE/CVF conference on computer vision and pattern recognition, pages 6700–6709, 2019.
- [20] Aaron Hurst, Adam Lerer, Adam P Goucher, Adam Perelman, Aditya Ramesh, Aidan Clark, AJ Ostrow, Akila Welihinda, Alan Hayes, Alec Radford, et al. Gpt-4o system card. arXiv preprint arXiv:2410.21276, 2024.
- [21] Alexander Kirillov, Eric Mintun, Nikhila Ravi, Hanzi Mao, Chloe Rolland, Laura Gustafson, Tete Xiao, Spencer Whitehead, Alexander C Berg, Wan-Yen Lo, et al. Segment anything. In Proceedings of the IEEE/CVF international conference on computer vision, pages 4015–4026, 2023.
- [22] Takeshi Kojima, Shixiang Shane Gu, Machel Reid, Yutaka Matsuo, and Yusuke Iwasawa. Large language models are zero-shot reasoners. Advances in neural information processing systems, 35:22199–22213, 2022.
- [23] Ranjay Krishna, Yuke Zhu, Oliver Groth, Justin Johnson, Kenji Hata, Joshua Kravitz, Stephanie Chen, Yannis Kalantidis, Li-Jia Li, David A Shamma, et al. Visual genome: Connecting language and vision using crowdsourced dense image annotations. International journal of computer vision, 123:32–73, 2017.
- [24] Bo Li, Yuanhan Zhang, Dong Guo, Renrui Zhang, Feng Li, Hao Zhang, Kaichen Zhang, Peiyuan Zhang, Yanwei Li, Ziwei Liu, et al. Llava-onevision: Easy visual task transfer. arXiv preprint arXiv:2408.03326, 2024.
- [25] Junnan Li, Dongxu Li, Silvio Savarese, and Steven Hoi. Blip-2: Bootstrapping language-image pre-training with frozen image encoders and large language models. In International conference on machine learning, 2023.
- [26] Yanwei Li, Yuechen Zhang, Chengyao Wang, Zhisheng Zhong, Yixin Chen, Ruihang Chu, Shaoteng Liu, and Jiaya Jia. Mini-gemini: Mining the potential of multi-modality vision language models. arXiv:2403.18814, 2024.
- [27] Yifan Li, Yifan Du, Kun Zhou, Jinpeng Wang, Wayne Xin Zhao, and Ji-Rong Wen. Evaluating object hallucination in large vision-language models. arXiv:2305.10355, 2023.
- [28] Tsung-Yi Lin, Michael Maire, Serge Belongie, James Hays, Pietro Perona, Deva Ramanan, Piotr Dollár, and C Lawrence Zitnick. Microsoft coco: Common objects in context. In Computer vision—ECCV 2014: 13th European conference, zurich, Switzerland, September 6–12, 2014, proceedings, part v 13, pages 740–755. Springer, 2014.
- [29] Weifeng Lin, Xinyu Wei, Ruichuan An, Peng Gao, Bocheng Zou, Yulin Luo, Siyuan Huang, Shanghang Zhang, and Hongsheng Li. Draw-and-understand: Leveraging visual prompts to enable mllms to comprehend what you want, 2024.
- [30] Zhiwei Lin, Yongtao Wang, and Zhi Tang. Training-free open-ended object detection and segmentation via attention as prompts. arXiv preprint arXiv:2410.05963, 2024.
- [31] Haotian Liu, Chunyuan Li, Yuheng Li, and Yong Jae Lee. Improved baselines with visual instruction tuning. arXiv:2310.03744, 2023.
- [32] Haotian Liu, Chunyuan Li, Yuheng Li, Bo Li, Yuanhan Zhang, Sheng Shen, and Yong Jae Lee. Llava-next: Improved reasoning, ocr, and world knowledge, January 2024. URL <https://llava-vl.github.io/blog/2024-01-30-llava-next/>.
- [33] Haotian Liu, Chunyuan Li, Qingyang Wu, and Yong Jae Lee. Visual instruction tuning. Advances in neural information processing systems, 2024.
- [34] Anand Mishra, Shashank Shekhar, Ajeet Kumar Singh, and Anirban Chakraborty. Ocr-vqa: Visual question answering by reading text in images. In 2019 international conference on document analysis and recognition (ICDAR), pages 947–952. IEEE, 2019.
- [35] Maxime Oquab, Timothée Darcet, Théo Moutakanni, Huy Vo, Marc Szafraniec, Vasil Khalidov, Pierre Fernandez, Daniel Haziza, Francisco Massa, Alaaeldin El-Nouby, et al. Dinov2: Learning robust visual features without supervision. arXiv preprint arXiv:2304.07193, 2023.
- [36] Long Ouyang, Jeffrey Wu, Xu Jiang, Diogo Almeida, Carroll Wainwright, Pamela Mishkin, Chong Zhang, Sandhini Agarwal, Katarina Slama, Alex Ray, et al. Training language models to follow instructions with human feedback. Advances in neural information processing systems, 35:27730–27744, 2022.
- [37] Baolin Peng, Chunyuan Li, Pengcheng He, Michel Galley, and Jianfeng Gao. Instruction tuning with gpt-4. arXiv:2304.03277, 2023.

- [38] Leigang Qu, Haochuan Li, Tan Wang, Wenjie Wang, Yongqi Li, Liqiang Nie, and Tat-Seng Chua. Unified text-to-image generation and retrieval. [arXiv preprint arXiv:2406.05814](#), 2024.
- [39] Alec Radford, Jeffrey Wu, Rewon Child, David Luan, Dario Amodei, Ilya Sutskever, et al. Language models are unsupervised multitask learners. [OpenAI blog](#), 2019.
- [40] Alec Radford, Jong Wook Kim, Chris Hallacy, Aditya Ramesh, Gabriel Goh, Sandhini Agarwal, Girish Sastry, Amanda Askell, Pamela Mishkin, Jack Clark, et al. Learning transferable visual models from natural language supervision. In [International conference on machine learning](#), pages 8748–8763. PMLR, 2021.
- [41] Alec Radford, Jong Wook Kim, Chris Hallacy, Aditya Ramesh, Gabriel Goh, Sandhini Agarwal, Girish Sastry, Amanda Askell, Pamela Mishkin, Jack Clark, et al. Learning transferable visual models from natural language supervision. In [International conference on machine learning](#), pages 8748–8763. PMLR, 2021.
- [42] Jeff Rasley, Samyam Rajbhandari, Olatunji Ruwase, and Yuxiong He. Deepspeed: System optimizations enable training deep learning models with over 100 billion parameters. In [Proceedings of the 26th ACM SIGKDD international conference on knowledge discovery & data mining](#), pages 3505–3506, 2020.
- [43] Aleksandar Shtedritski, Christian Rupprecht, and Andrea Vedaldi. What does clip know about a red circle? visual prompt engineering for vlms. In [Proceedings of the IEEE/CVF International Conference on Computer Vision](#), pages 11987–11997, 2023.
- [44] Amanpreet Singh, Vivek Natarjan, Meet Shah, Yu Jiang, Xinlei Chen, Devi Parikh, and Marcus Rohrbach. Towards VQA models that can read. In [Proceedings of the IEEE Conference on Computer Vision and Pattern Recognition](#), pages 8317–8326, 2019.
- [45] Zeyi Sun, Ye Fang, Tong Wu, Pan Zhang, Yuhang Zang, Shu Kong, Yuanjun Xiong, Dahua Lin, and Jiaqi Wang. Alpha-clip: A CLIP model focusing on wherever you want. In [IEEE/CVF Conference on Computer Vision and Pattern Recognition, CVPR 2024, Seattle, WA, USA, June 16-22, 2024](#), pages 13019–13029, 2024.
- [46] Gemini Team, Petko Georgiev, Ving Ian Lei, Ryan Burnell, Libin Bai, Anmol Gulati, Garrett Tanzer, Damien Vincent, Zhufeng Pan, Shibo Wang, et al. Gemini 1.5: Unlocking multimodal understanding across millions of tokens of context. [arXiv preprint arXiv:2403.05530](#), 2024.
- [47] Hugo Touvron, Thibaut Lavril, Gautier Izacard, Xavier Martinet, Marie-Anne Lachaux, Timothée Lacroix, Baptiste Rozière, Naman Goyal, Eric Hambro, Faisal Azhar, et al. Llama: Open and efficient foundation language models. [arXiv:2302.13971](#), 2023.
- [48] Hugo Touvron, Louis Martin, Kevin Stone, Peter Albert, Amjad Almahairi, Yasmine Babaei, Nikolay Bashlykov, Soumya Batra, Prajwal Bhargava, Shrutu Bhosale, et al. Llama 2: Open foundation and fine-tuned chat models. [arXiv preprint arXiv:2307.09288](#), 2023.
- [49] Jason Wei, Xuezhi Wang, Dale Schuurmans, Maarten Bosma, Fei Xia, Ed Chi, Quoc V Le, Denny Zhou, et al. Chain-of-thought prompting elicits reasoning in large language models. [Advances in neural information processing systems](#), 35:24824–24837, 2022.
- [50] Junda Wu, Xintong Li, Tong Yu, Yu Wang, Xiang Chen, Jiuxiang Gu, Lina Yao, Jingbo Shang, and Julian McAuley. Commit: Coordinated instruction tuning for multimodal large language models. [arXiv preprint arXiv:2407.20454](#), 2024.
- [51] Junda Wu, Zhehao Zhang, Yu Xia, Xintong Li, Zhaoyang Xia, Aaron Chang, Tong Yu, Sungchul Kim, Ryan A Rossi, Ruiyi Zhang, et al. Visual prompting in multimodal large language models: A survey. [arXiv preprint arXiv:2409.15310](#), 2024.
- [52] Junbin Xiao, Angela Yao, Yicong Li, and Tat-Seng Chua. Can i trust your answer? visually grounded video question answering. In [Proceedings of the IEEE/CVF Conference on Computer Vision and Pattern Recognition](#), pages 13204–13214, 2024.
- [53] Lingfeng Yang, Yueze Wang, Xiang Li, Xinlong Wang, and Jian Yang. Fine-grained visual prompting. [Advances in Neural Information Processing Systems](#), 36:24993–25006, 2023.
- [54] Senqiao Yang, Yukang Chen, Zhuotao Tian, Chengyao Wang, Jingyao Li, Bei Yu, and Jiaya Jia. Visionzip: Longer is better but not necessary in vision language models. [arXiv preprint arXiv:2412.04467](#), 2024.
- [55] Runpeng Yu, Weihao Yu, and Xinchao Wang. Attention prompting on image for large vision-language models. In [European Conference on Computer Vision](#), pages 251–268. Springer, 2024.

- [56] Sicheng Yu, Chengkai Jin, Huanyu Wang, Zhenghao Chen, Sheng Jin, Zhongrong Zuo, Xiaolei Xu, Zhenbang Sun, Bingni Zhang, Jiawei Wu, et al. Frame-voyager: Learning to query frames for video large language models. [arXiv preprint arXiv:2410.03226](#), 2024.
- [57] Weihao Yu, Zhengyuan Yang, Linjie Li, Jianfeng Wang, Kevin Lin, Zicheng Liu, Xinchao Wang, and Lijuan Wang. Mm-vet: Evaluating large multimodal models for integrated capabilities. [arXiv preprint arXiv:2308.02490](#), 2023.
- [58] Xiang Yue, Yuansheng Ni, Kai Zhang, Tianyu Zheng, Ruoqi Liu, Ge Zhang, Samuel Stevens, Dongfu Jiang, Weiming Ren, Yuxuan Sun, et al. Mmmu: A massive multi-discipline multimodal understanding and reasoning benchmark for expert agi. In [Proceedings of the IEEE/CVF Conference on Computer Vision and Pattern Recognition](#), pages 9556–9567, 2024.
- [59] Xiaohua Zhai, Basil Mustafa, Alexander Kolesnikov, and Lucas Beyer. Sigmoid loss for language image pre-training. In [Proceedings of the IEEE/CVF international conference on computer vision](#), pages 11975–11986, 2023.
- [60] Ao Zhang, Hao Fei, Yuan Yao, Wei Ji, Li Li, Zhiyuan Liu, and Tat-Seng Chua. Vpgrans: Transfer visual prompt generator across llms. [Advances in Neural Information Processing Systems](#), 36:20299–20319, 2023.
- [61] Chao Zhang, Weiming Li, Wanli Ouyang, Qiang Wang, Woo-Shik Kim, and Sunghoon Hong. Referring expression comprehension with semantic visual relationship and word mapping. In [Proceedings of the 27th ACM International Conference on Multimedia](#), pages 1258–1266, 2019.
- [62] Shaolei Zhang, Qingkai Fang, Zhe Yang, and Yang Feng. Llava-mini: Efficient image and video large multimodal models with one vision token. [arXiv preprint arXiv:2501.03895](#), 2025.
- [63] Yuan Zhang, Chun-Kai Fan, Junpeng Ma, Wenzhao Zheng, Tao Huang, Kuan Cheng, Denis Gudovskiy, Tomoyuki Okuno, Yohei Nakata, Kurt Keutzer, et al. Sparsevlm: Visual token sparsification for efficient vision-language model inference. [arXiv preprint arXiv:2410.04417](#), 2024.
- [64] Yuan Zhang, Tao Huang, Chun-Kai Fan, Hongyuan Dong, Jiawen Li, Jiacong Wang, Kuan Cheng, Shanghang Zhang, Haoyuan Guo, et al. Unveiling the tapestry of consistency in large vision-language models. [Advances in Neural Information Processing Systems](#), 37:118632–118653, 2024.
- [65] Kaiyang Zhou, Jingkang Yang, Chen Change Loy, and Ziwei Liu. Conditional prompt learning for vision-language models. In [IEEE/CVF Conference on Computer Vision and Pattern Recognition \(CVPR\)](#), 2022.
- [66] Zhuofan Zong, Bingqi Ma, Dazhong Shen, Guanglu Song, Hao Shao, Dongzhi Jiang, Hongsheng Li, and Yu Liu. Mova: Adapting mixture of vision experts to multimodal context. [arXiv preprint arXiv:2404.13046](#), 2024.

Appendix

A Attention Visual Prompts used in Experiments

Alignment in Vision Foundation Models. As vision foundation models advance rapidly [21, 35, 40, 59], pretrained on language-image pairs, they serve as the visual encoders for large vision-language models. A representative model is CLIP [40], $g_{\text{CLIP}}(\cdot)$, which consists of a vision encoder and a text encoder, mapping the image and text prompt into the aligned latent space. Therefore, we can directly obtain the similarity \mathbf{S} between vision modality \mathbf{I} and text modality feature \mathbf{T} with $\mathbf{S} = g_{\text{CLIP}}(\mathbf{I}, \mathbf{T})$.

Attention Visual Prompts. Inspired by the idea that text-image attention (or similarity) \mathbf{S} can be visualized as visual prompts for LVLMs [30, 55], where similarity heatmaps overlaid on the image highlight key regions requiring greater attention for prompt-based reasoning. In this work, we adopt a fine-grained similarity visualization manner in API [55], with the l -th layer similarity \mathbf{S}^l defined as follows:

$$\mathbf{S}^l = \text{SIM}(\mathbf{I}^l, \mathbf{T}) \approx \sum_{i=l}^L \sigma([\text{MSA}^i(\mathbf{Z}^{i-1})]_{\text{cls}}) \times \mathbf{T}, \quad (5)$$

where L denotes the number of transformer layers, σ is the projection layer with a fully-connected layer and normalization operation, and MSA stands for multi-head self-attention structure. \mathbf{Z}^l is input vision tokens for the l -th layer, while $[\mathbf{Z}]_{\text{cls}}$ indicates the class token in the token sequence \mathbf{Z} .

B Training Data

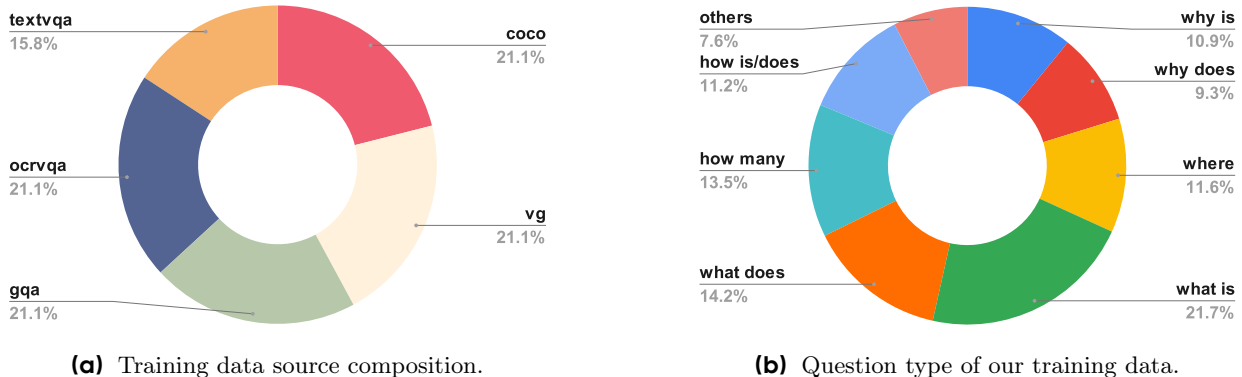


Figure 6 Visual analysis of the composition of our training data. Best viewed in color.

Our training source dataset is composed of several components used in LLaVA [31] to ensure that AutoV is trained on a diverse range of image-question pairs. It includes 25K samples from the COCO train dataset [28], 20K samples from the Visual Genome (VG) dataset [23], 20K samples from the GQA dataset [19], 20K samples from the OCRVQA dataset [34], and 15K samples from the TextVQA dataset [44]. In total, the source data contains 100K image-question pairs. Here, we visualize the proportional relationship of the source dataset in Figure 6 (a). Furthermore, the question types in our training dataset in visualized in Figure 6 (b), and the selected data types are relatively balanced, which enhances the generalizability and robustness of the ranking network in AutoV.

We then generate various visual prompts based on the above source data. Here, we simply use the **attention prompting** method employed by the API [55] for high-quality generation. To streamline the process, we empirically generate heat maps of attention maps corresponding to CLIP [40] layers 15, 20, 22, and 23 under its setting on the image as our training visual prompts. A specific example (including JSON dictionary and images) can be found in Figure 7. As a result, one question will correspond to four visual prompts, with a total of AutoV being trained on 40K visual prompts.

C Evaluation Benchmarks

We conducted experiments on several widely used visual understanding benchmarks.

MMMU. [58] The MMMU is designed to evaluate large vision-language models across a wide range of academic disciplines and complex tasks. It covers over 30 subjects including history, medicine, physics, and more, requiring multimodal comprehension, fine-grained reasoning, and domain-specific knowledge. Each question in MMMU is paired with an image and a multiple-choice question, testing the model’s ability to integrate visual understanding with deep textual reasoning.

GQA. [19] The GQA benchmark is composed of three parts: scene graphs, questions, and images. The image part contains images, as well as the spatial features of images and the features of all objects in images. The questions in GQA are designed to test the understanding of visual scenes and the ability to reason about different aspects of an image.

POPE. [27] The POPE benchmark is primarily used to evaluate the degree of Object Hallucination in models. It reformulates hallucination evaluation by requiring the model to answer a series of specific binary questions regarding the presence of objects in images. Accuracy, Recall, Precision, and F1 Score are effectively employed as reliable evaluation metrics to precisely measure the model’s hallucination level under three different sampling strategies.

TextVQA. [44] The TextVQA benchmark focuses on the comprehensive integration of diverse text information within images. It meticulously evaluates the model’s text understanding and reasoning abilities through a series of visual question-answering tasks with rich textual information. Models need to not only understand the visual content of the images but also be able to read and reason about the text within the images to answer the questions accurately.

MMVet. [57] The MMVet benchmark is designed based on the insight that the intriguing ability to solve complicated tasks is often achieved by a generalist model being able to integrate different core vision-language capabilities. MM-Vet defines 6 core VL capabilities and examines the 16 integrations of interest derived from the capability combination.

LLaVA-In-The-Wild. [31] The LLaVA-In-The-Wild benchmark is built to assess the generalization ability of vision-language models in real-world, unconstrained settings. Unlike curated benchmarks, it features user-collected image-question pairs from diverse sources and domains. This setup presents models with noisy, complex, and unpredictable visual content, offering a realistic measure of their robustness, grounding capability, and performance in open-ended scenarios.

D Implementation Details.

(1) Data generation stage: LLaVA-v1.5 is consistently adopted as the reference LVLm for generating loss due to resource limitations. (2) AutoV training stage: LLaVA series are trained using DeepSpeed [42] ZeRO2 with 8 A100-40G GPUs within 40 epochs. The batch size (with accumulation) is set to 64 and the learning rate is $1e-3$. For convenience, Qwen2.5-VL and InternVL2 directly adopt the retrieval strategy in AutoV pre-trained from LLaVA-OneVision.

E Limitations

The introduced AutoV offers a new perspective on retrieving various visual prompts for LVLms when faced with different queries. However, due to resource constraints, we only generate the training data via LLaVA-7B model [31], and AutoV might yield superior results with more powerful large vision-language models. Besides, to maintain parameter efficiency, we design our approach as a plug-in module for existing LVLms, requiring no fine-tuning of the model. We note, however, that naively reusing the LLM frozen parameters may lead to suboptimal performance. Finally, due to current limitations in visual prompt quality, our selection is constrained to attention visual prompts [55], resulting in bounded accuracy gains. We believe that when future advances in visual prompt generation, AutoV can further boost their integrated performance.

F Broader Impacts

Overall, this research has broader impacts on the visual prompt, feature retrieval, and future development of LVLMs, fostering progress and advancements in the field of vision-language models.

Advancing Method: We propose the AutoV model that learns to automatically select the optimal visual prompt from various candidates based on given textual queries and the input image.

Novel Insights: We are the first to apply the reward modeling loss from RLHF [41] to optimal visual prompt retrieval and validate its effectiveness compared with the Mixture-of-Experts framework.

Inspiring Future Research: This work advances visual prompt retrieval in LVLMs, establishing a foundation for future research. By framing the prompt selection challenge systematically, we enable subsequent exploration of (1) higher-quality prompt generation techniques and (2) more effective retrieval methodologies, collectively pushing the boundaries of multimodal understanding.

G More Visualization

G.1 Cases of Training Data

Visualization of a case in our training data is in Figure 7, including a JSON dictionary and images.

G.2 Retrieval Strategy of AutoV

Visualization of the retrieval strategy employed by AutoV is in Figure 5, with a total of ten cases.



Figure 7 Visualization of a training sample. Best viewed in color.

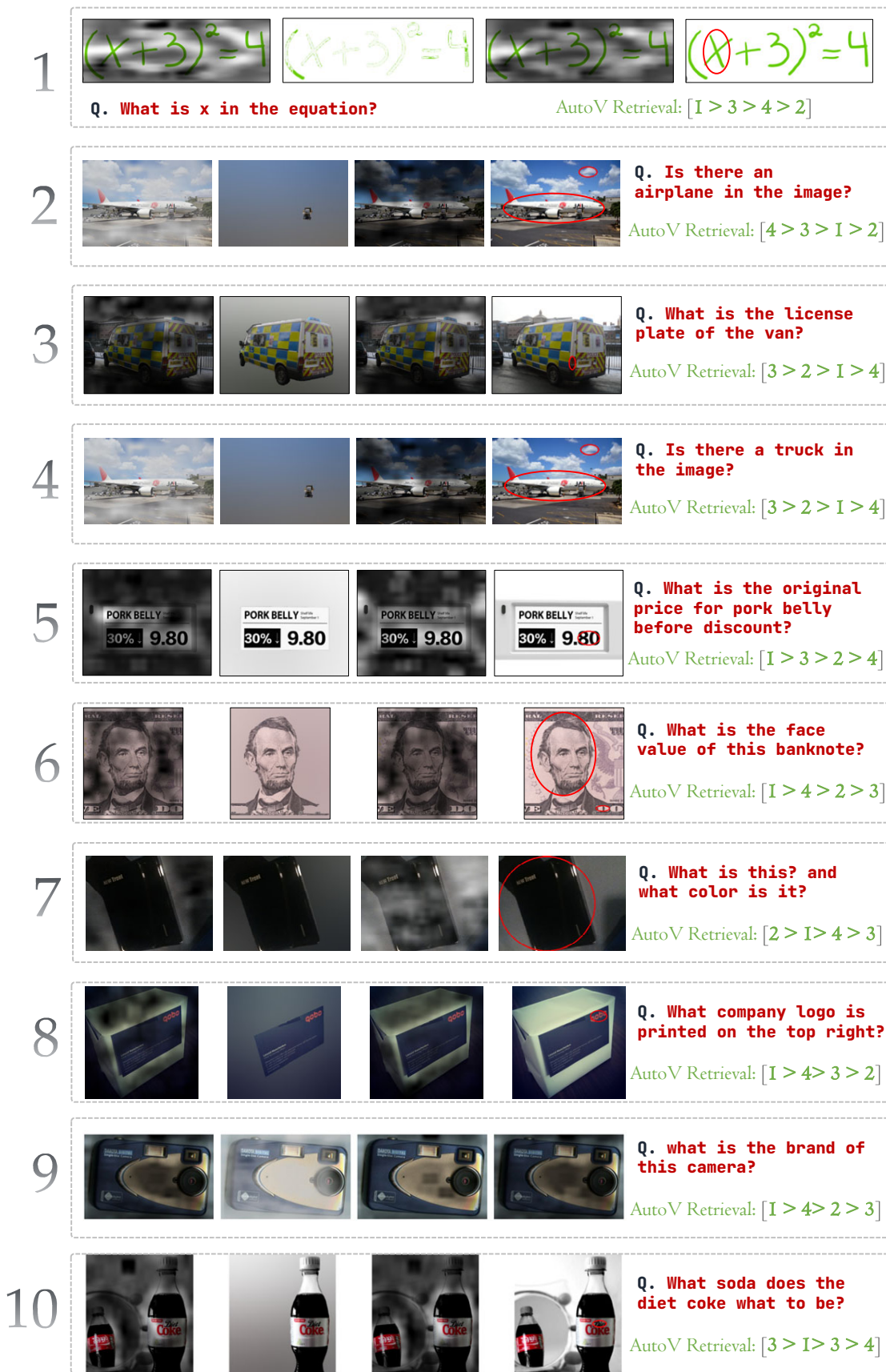


Figure 8 Visualization of visual prompts ranked by AutoV. Best viewed in color.